

Analytical design technique for real-to-real single- and dual-frequency impedance matching networks in lossy passive environment

Aravinth Kumar A.R.¹ ✉, Shiv Govind Singh¹, Ashudeb Dutta¹

¹Department of Electrical Engineering, Indian Institute of Technology Hyderabad, Kandi, Medak, Telangana 502285, India

✉ E-mail: ee10p001@iith.ac.in

ISSN 1751-8725

Received on 20th August 2017

Revised 27th November 2017

Accepted on 2nd January 2018

E-First on 20th March 2018

doi: 10.1049/iet-map.2017.0780

www.ietdl.org

Abstract: A passive-loss accounted analytic design technique for impedance matching networks is proposed here for efficient radio frequency (RF) circuit design. The impact of component losses on matching performance is briefed initially. To overcome the matching impact due to component losses, a set of modified equations are introduced which finds the accurate inductor and capacitor values accounting component losses. The proposed technique is applied for single-frequency L-match, Pi-match, T-match and dual-frequency L-match networks. The improvement in matching performance by using the proposed design technique is validated through simulations and measurements in UMC 0.18 μm complementary metal oxide semiconductor technology. The measurement results closely (90–95%) follow ideal component performance. Hence, the proposed passive-loss accounted design technique will be more useful in accurate low power RF circuit design.

1 Introduction

Presently, the use of radio frequency (RF) systems is growing rapidly in wide range of single- and multi-frequency applications with stringent specifications like sensitivity and selectivity. Impedance matching is one of the key factors in these systems which helps to reduce reflections and increase efficiency [1, 2]. Matching networks find useful applications in low noise amplifiers and power amplifiers [3], resonant inverters, rectifiers, DC–DC converters [4], RF energy harvesting circuits, and in preventing electromagnetic interference in high-speed electronic circuits [5]. Their implementation in complementary metal oxide semiconductor (CMOS) technologies has attracted more research interest to realise compact system-on-chip (SoC) solution. There exists different circuit topologies for impedance matching purpose [6, 7] and L, Pi, and T matching networks are commonly used ones. The type of matching network is chosen depending on various design requirements such as source and load resistances, passband type (lowpass, highpass, bandpass, and bandstop), operating bandwidth etc. Considering easy implementation and less number of components, L-network is more preferred where bandwidth control is not needed. On the other hand, Pi and T networks are chosen where control on matching bandwidth is required [8]. Numerous lumped and distributed circuit techniques are proposed in the literature to implement matching networks. Further, for SoC implementation, these networks need to be incorporated on-chip, where lumped element approximation is valid and acceptable within few gigahertz (GHz) frequencies. The generic design approach in the literature for these matching networks considers the passive components are non-lossy and ideal. However, the Q -factor of inductors in present CMOS technologies is finite and even low value. In few of the low cost CMOS technologies, the value is below ten. Therefore, if a circuit is designed assuming that the components are ideal, the practical performance will deviate from the ideal one, requiring typical post-fabrication tuning and also makes performance deviations. To rectify this issue, literatures proposed multiple solutions such as process-invariant design approach [9], efficient matching [4], Q -based design [5], reconfigurable matching [10], adaptive matching [11], high gain power matching [12], automatic matching network [13], lumped lossy numerical circuit synthesis [14, 15] etc. Though these approaches perform good in real time, they are highly complex circuits and require more hardware. This leads to higher

cost and implementation time. Furthermore, there is no analytical design method exists for lumped matching networks accounting for their parasitic losses. In this paper, we propose a passive-loss aware analytical design technique for real-to-real single- and dual-frequency impedance matching networks. For explanation purpose, our proposed technique is applied in single-frequency L, Pi, and T match networks and dual-frequency L-match networks. However, this technique can be extended to other networks as well. The rest of this paper is organised as follows. Section 2 briefs the matching networks design basics and the impact of losses associated with passive components. The proposed technique for L, Pi, T match networks and dual-frequency L-match network are explained in Sections 3–6, respectively. An example design of Pi and dual-frequency L-networks and their measurement results are discussed in Section 7.

2 Impedance matching networks and impact of component losses

Impedance matching networks (in form of L, Pi, and T) had been discussed in numerous text books and articles, for example [7]. Most of these literatures consider the passive components are ideal irrespective of the fact that, these components are fabricated either on insulating (FR4), semi-insulating (GaAs), or conducting (CMOS) substrates. Owing to substrate losses and other parasitic (high in CMOS technologies), equivalent circuit of the passive components become complex which degrades the component Q -factor. Also the component Q -factor is frequency-dependent. However, at any given frequency point, these components can be represented as single equivalent inductance (or capacitance) and series resistance (or parallel conductance) with a finite Q value, whose approximate values are obtained from process design kit (PDK) or using small signal simulations. These losses (finite Q) strongly impact the matching performance of the circuit. The basic piece of any impedance matching circuit, the L-network is considered here, and its performance impact due to its passive losses are detailed at first. To demonstrate, the matching performance of L-network with and without accounting component losses are plotted in terms of input reflection coefficient (S_{11}) as shown in Fig. 1 (component values to match from 20 to 50 Ω are tabulated in Table 1). From Fig. 1, it is very clear that, for circuits with low- Q passives ($Q_L = 5$, $Q_C = 30$), the input matching

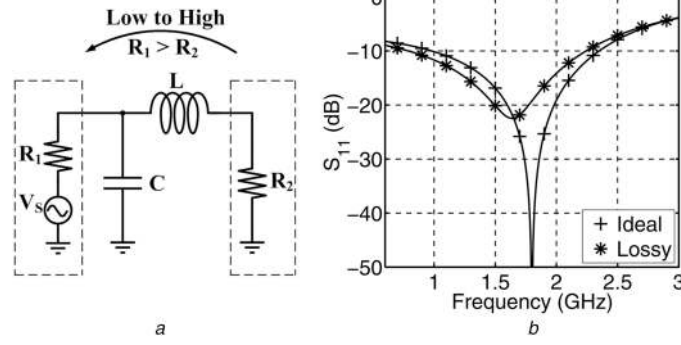


Fig. 1 Impact of parasitics on matching performance

(a) Low to high (LtoH) L-match circuit, (b) Input reflection (S_{11}) plot of an ideal circuit designed to match from 20 to 50 Ω at 1.8 GHz

degrades in terms of poor input reflection at the frequency of interest as well as shift in the designed frequency. Though the impact is shown only for L-network, these impact are same or even worse in other networks. Therefore, the component losses must be accounted for, in any matching circuit design to overcome these effects. In the following sections, we formulate the design technique for L-match network design accounting for component losses and the same is extended to Pi, T, and dual-band L-networks in further sections.

3 Loss accounted L-match network design

The circuit diagram of an ideal low-to-high low pass L-matching network is shown in Fig. 2a and the impedance equation for the same is given by the below equation

$$\frac{1}{R_1} = \frac{1}{R_2 + jX_L} - \frac{1}{jX_C} \quad (1)$$

Solution for this circuit in ideal case is derived on the basis of quality factors of series and parallel sections at the frequency of interest (ω_0) as shown below (2)

$$Q_S = Q_P = \sqrt{\frac{R_1}{R_2} - 1} \quad (2)$$

where

$$Q_P = \frac{R_1}{X_C} \text{ and } Q_S = \frac{X_L}{R_2} \quad (3)$$

As briefed in the previous section and Fig. 1, if these equations are used for on-chip network design, the performance degradation becomes unavoidable. To overcome the parasitic impacts, Dasgupta *et al.* [16] included the non-ideal effects and proposed an analytical design approach for L-matching network. The parasitic resistance of passive components can be represented in terms of their quality factors at the frequency of interest as given by the below equation

$$R_L = \frac{X_L}{Q_L}, \quad R_C = \frac{X_C}{Q_C} \text{ or } G_C = \frac{1}{X_C} \left(\frac{Q_C}{1 + Q_C^2} \right) \quad (4)$$

A low-to-high low pass L-matching network accounting for the component parasitics is shown in Fig. 2b. Including component parasitics, the impedance equation of this circuit in terms of inductor and capacitor quality factors (Q_L and Q_C) becomes

$$\frac{1}{R_1} = \frac{1}{(R_2 + jX_L + (X_L/Q_L))} + \frac{1}{((X_C/Q_C) - jX_C)} \quad (5)$$

Solution for this modified circuit is derived by separating real and imaginary part of (5) and equating both sides. Component values are found by solving these two equations given by (6) and (7)

$$\begin{aligned} & \left[(R_2 - R_1) \left(1 + \frac{1}{Q_C^2} \right) \right] |X_C|^2 \\ & + \left[R_1^2 \left(\frac{1}{Q_L} + \frac{1}{Q_C} \right) + \left(\frac{2R_1}{Q_C} - R_2 \right) \right] |X_C| \\ & + R_2 R_1^2 = 0 \end{aligned} \quad (6)$$

$$X_L = \frac{R_1 X_C - X_C R_2}{R_1 + (X_C/Q_L) - (X_C/Q_C)} \quad (7)$$

This method can be extended to other L-matching networks as well. The design equations derived for a high-to-low low-pass L-matching network are given below

$$\begin{aligned} & \left[(R_1 Q_L - R_2 Q_L) \left(1 + \frac{1}{Q_C^2} \right) \right] |X_C|^2 \\ & + \left[\frac{2R_1 Q_L R_2}{Q_C} - R_2^2 \left(1 + \frac{Q_L}{Q_C} \right) \right] |X_C| \\ & + R_1 Q_L R_2^2 = 0 \end{aligned} \quad (8)$$

$$X_L = \frac{((-X_C^2 R_2)/Q_C) + X_C R_2 (R_2 + (X_C/Q_C))}{(R_2 + (X_C/Q_C)) + (-X_C)^2} \quad (9)$$

A set of component values to match from 20 to 50 Ω and 50 to 20 Ω at 1.8 GHz frequency are computed and are listed in Table 2. From Table 2, it has been observed that, commendable changes in component values are essential (>50%) when component quality factor degrades from infinite (ideal) to below ten. The S_{11} and S_{21} performances of the circuits using these components are plotted in Fig. 3. From the figure, it is proven that the proposed solution gives much better (close to ideal) matching even with low Q -factor components.

4 Passive-loss accounted Pi-match network design

One of the drawbacks in L-matching network is its inability to control the matching bandwidth, which is defined only by source and load impedances as given in the below equation

$$Q_{Lmatch} = \sqrt{\frac{R_S}{R_L} - 1}, \quad \text{where } R_S > R_L \quad (10)$$

To get control over matching bandwidth, Pi or T network is formed by introducing an additional element in L-network. The passive-loss accounted design of Pi-matching network is explained below.

The design of Pi-matching network is done by splitting the circuit into two suitable L-sections and the corresponding design equations for a given transformation quality factor (Q_{IN}) are given in (11)–(13) [7]

$$L = L_R + L_L = \frac{(Q_{right} + Q_{left})R_I}{\omega_0} = \frac{Q_{IN}R_I}{\omega_0} \quad (11)$$

Table 1 Derived component values for ideal circuits at 1.8 GHz

CKT	L (nH)	C (pF)
L-match (L-to-H)	2.166	2.166
L-match (H-to-L)	2.166	2.166

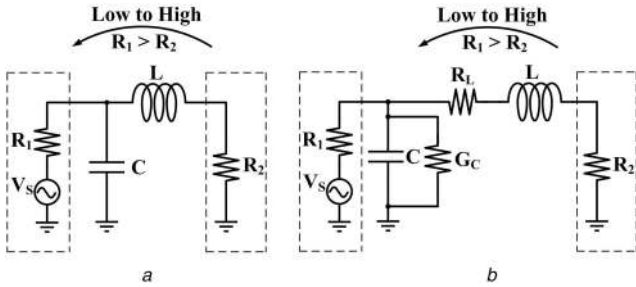


Fig. 2 Low-to-high low-pass L-match network (a) Ideal circuit, (b) Practical circuit

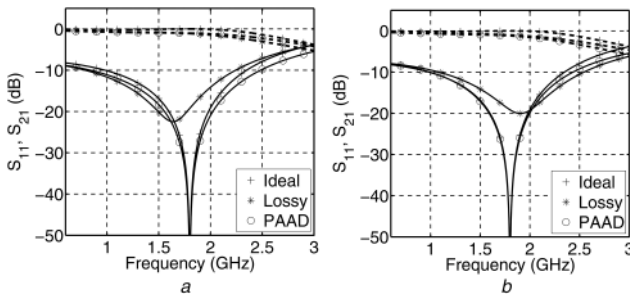


Fig. 3 S_{11} and S_{21} response of L-match network using the proposed design technique. Solid lines are S_{11} and dotted lines are S_{21} (a) Low-to-high network, (b) High-to-low network

$$Q_{IN} = Q_{right} + Q_{left} = \sqrt{\frac{R_2}{R_I} - 1} + \sqrt{\frac{R_1}{R_I} - 1} \quad (12)$$

$$C_R = \frac{Q_{right}}{\omega_0 R_2} \quad \text{and} \quad C_L = \frac{Q_{left}}{\omega_0 R_1} \quad (13)$$

where R_I is the intermediate impedance, Q_{left} and Q_{right} are quality factor of the left and right L-matching networks, respectively, ω_0 is the matching frequency, R_1 and R_2 are the source and load impedances, respectively. The parasitic aware L-matching network (above discussed) can be adapted here as well for designing individual L-matching network. However, choice of the networks is to be analysed. For a Pi-matching network, four possible L-matching combinations can be availed as below

- i. high-to-low (Left-L), low-to-high (Right-L);
- ii. high-to-low (Left-L), high-to-low (Right-L);
- iii. low-to-high (Left-L), low-to-high (Right-L);
- iv. low-to-high (Left-L), high-to-low (Right-L).

Among these, option (iv) is the only suitable solution while accounting for the component losses. This is due to the variation appears in the impedance after matching, on individual L-matching circuits. In detail, when the components are lossy, an L-matching network should be computed in the same way that need to be matched (connected or measured). In lossy component environment, the matching is not reversible, i.e. match from R_1 to R_2 does not lead to the same component values as for R_2 to R_1 . This is clear from Table 2, where the component values are different for 20–50 Ω matching and 50–20 Ω matching in low- Q case. Hence, if the circuit is designed in reverse direction, the resulting total impedance will be unmatched. Fig. 4 shows the variation in impedance between the forward computed and reverse computed cases over different quality factor values of inductor and capacitor.

Table 2 Derived component values for L-match network at 1.8 GHz

	20–50 Ω		50–20 Ω	
Q_L, Q_C	∞, ∞	5, 30	∞, ∞	5, 30
L	2.166 nH	2.233 nH	2.166 nH	2.02 nH
C	2.166 pF	1.765 pF	2.166 pF	2.658 pF

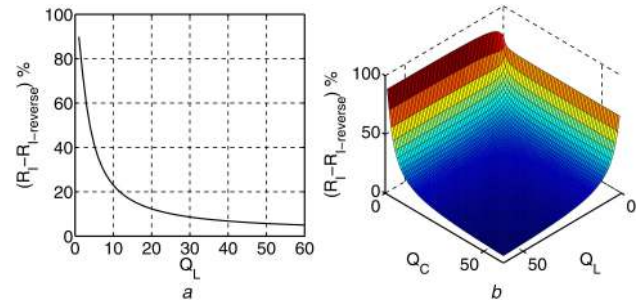


Fig. 4 Reverse matching impact (impedance variation) over component quality factor (a) With respect to inductor quality factor, (b) With respect to inductor and capacitor quality factor

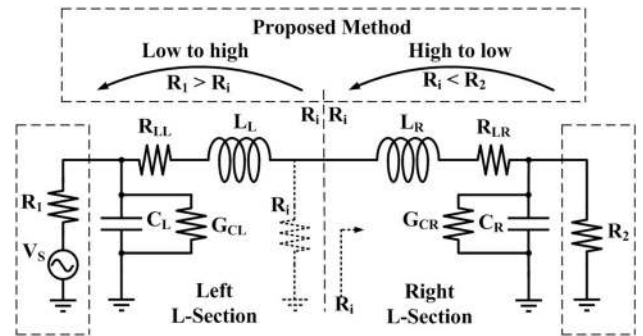


Fig. 5 Synthesised Pi-matching network

The variation is more prominent for poor quality factor components.

For any transformation quality factor (Q_{IN}), the intermediate impedance (R_I) will be less than that of source and load impedances. Hence, for a Pi-matching network, the right L-section has to be considered as high-to-low L-match and the left one as low-to-high L-matching network as shown in Fig. 5. After calculating component values for individual L-networks, the two inductors are added together ($L = L_L + L_R$) to create a three element Pi network. Applying this method, a Pi-matching network is designed to match from 20 to 50 Ω at different frequencies and the corresponding component values are listed in Table 3. The S_{11} and S_{21} performance of Pi-matching network using these components is compared with ideal and lossy components performance at 1.8 and 2.4 GHz centre frequencies as shown in Fig. 6. Fig. 6 proves that the proposed approach nullifies the parasitic impact and closely follows the ideal S_{11} response. From Table 3, it is clear that the component values have to be changed (>50%) while using low Q -factor components. This is validated through Fig. 6.

5 Parasitic aware T-matching network design

A low-pass T-match network is dual of Pi-match network described in the previous section. Hence, synthesis of T-match network is done in the same way as Pi-matching network by splitting the circuit into two L-sections and solving them individually.

Assuming all the components are ideal, the design equations are given in (14)–(16)

$$C = C_R + C_L = \frac{(Q_{right} + Q_{left})R_I}{\omega_0} = \frac{Q_{in}}{\omega_0 R_I} \quad (14)$$

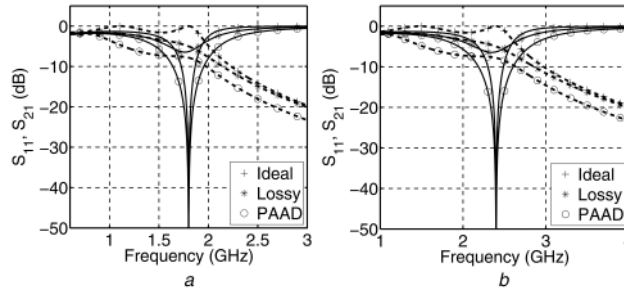


Fig. 6 S_{11} and S_{21} response of Pi-match network with derived components. Solid lines are S_{11} and dotted lines are S_{21} (a) Designed for 1.8 GHz, (b) Designed for 2.4 GHz

Table 3 Derived component values for Pi-matching network

Comp	Q_L, Q_C	0.9 G	1.8 G	2.1 G	2.4 G
L_L , nH	∞, ∞	1.55	0.78	0.67	0.58
	5, 30	2.72	1.36	1.16	1.02
L_R , nH	∞, ∞	0.95	0.47	0.40	0.35
	5, 30	0.65	0.32	0.29	0.24
$L = L_L + L_R$, nH	∞, ∞	2.5	1.25	1.07	0.93
	5, 30	3.37	1.68	1.45	1.26
C_L , pF	∞, ∞	19.52	9.76	8.37	7.32
	5, 30	10.57	5.28	4.53	3.96
C_R , pF	∞, ∞	30.52	15.26	13.08	11.45
	5, 30	45.91	22.95	19.67	17.22

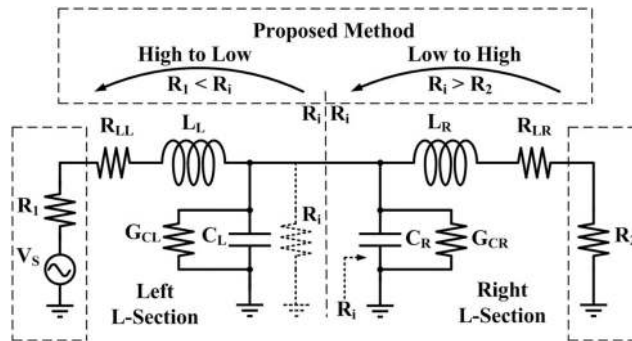


Fig. 7 Synthesised T-matching network

Table 4 Derived component values for T matching network

Comp	Q_L, Q_C	0.9 G	1.8 G	2.1 G	2.4 G
L_L , nH	∞, ∞	30.21	15.11	12.95	11.33
	5, 30	20.75	10.37	8.89	7.78
L_R , nH	∞, ∞	19.85	9.92	8.51	7.44
	5, 30	34.74	17.37	14.89	13.03
C_L , pF	∞, ∞	0.95	0.48	0.41	0.36
	5, 30	1.44	0.72	0.62	0.554
C_R , pF	∞, ∞	1.52	0.76	0.65	0.57
	5, 30	0.83	0.41	0.35	0.31
$C = C_L + C_R$, pF	∞, ∞	2.47	1.24	1.06	0.93
	5, 30	2.27	1.13	0.97	0.864

$$Q_{IN} = Q_{right} + Q_{left} = \sqrt{\frac{R_I}{R_2} - 1} + \sqrt{\frac{R_I}{R_1} - 1} \quad (15)$$

$$L_R = \frac{R_2 Q_{right}}{\omega_0} \quad \text{and} \quad L_L = \frac{R_1 Q_{left}}{\omega_0} \quad (16)$$

For a T-matching network, the intermediate impedance (R_I) is always greater than the source and load impedance (R_1, R_2). Hence, in the proposed technique, the left half L-section has to be considered as high-to-low matching network and right half L-

section has to be considered as low-to-high matching network as shown in Fig. 7. After calculating the component values for individual L-networks, the two capacitance values are added together ($C = C_L + C_R$) to form a three element T-match network.

Table 4 lists a set of component values derived using the proposed method for 20 Ω (load) to 50 Ω (source) matching at different frequencies. The S_{11} and S_{21} performance of T-matching network is compared with ideal and lossy component behaviour for 1.8 and 2.4 GHz centre frequencies and are shown in Fig. 8. From Fig. 8, it is evident that the response of the proposed technique closely follows the ideal component performance.

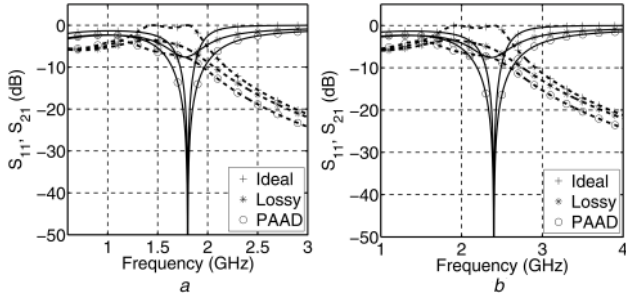


Fig. 8 S_{11} and S_{21} response of T-matching network with derived components. Solid lines are S_{11} and dotted lines are S_{21}
(a) Designed for 1.8 GHz, (b) Designed for 2.4 GHz

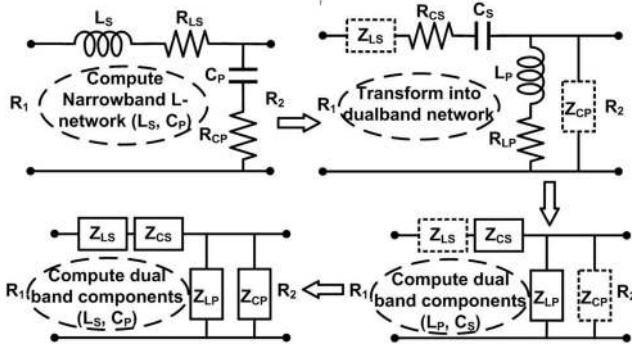


Fig. 9 Flowchart of parasitic aware concurrent dual-band matching circuit

The proposed analytical design technique nullifies the effect of non-idealities on L, Pi, and T matching networks and provides matching performance close (90–95%) to ideal one. A little degradation seen in insertion loss is due to increased inductor values obtained from the proposed design method. However, the finest improvement in input reflection overcomes this effect, and makes overall performance close to ideal.

6 Parasitic aware dual-frequency L-match network

The design of dual-band network also follow a similar procedure as explained in previous sections. In the proposed method for dual-band networks (design flow shown in Fig. 9), initially components (L_S and C_P) of a narrow band L-network including component parasitics are derived using following set of (17), (18) for a resonance frequency of $\omega_0 = |\omega_1 - \omega_2|$, where ω_1, ω_2 are required frequencies

$$X_{LS}^2 \left(1 + \frac{1}{Q_L^2}\right) + X_{LS} \left[\frac{2R_2}{Q_L} - R_1 \left(\frac{1}{Q_L} + \frac{1}{Q_C}\right)\right] - R_2^2 Q^2 = 0 \quad (17)$$

$$X_{CP}^2 \left(1 + \frac{1}{Q_C^2}\right) + X_{CP} \left(\frac{Q^2 + 1}{Q^2}\right) \times \left[\frac{2R_2}{Q_C} - R_1 \left(\frac{1}{Q_L} + \frac{1}{Q_C}\right)\right] - \frac{R_1^2}{Q^2} = 0 \quad (18)$$

where $Q = \sqrt{(R_2/R_1) - 1}$ is the system quality factor.

Next, this L-matching network is transformed into a concurrent dual-band network using the frequency transformation method [17]. The new input impedance of the network including component parasitics becomes (see (19) and (20)). Since two components (L_S and C_P) have been computed earlier, the two unknown components (L_P and C_S) are calculated from a set of quadratic (20), (21) derived by splitting the real and imaginary part of the impedance (19) for the frequency $\omega_0 = \sqrt{\omega_1 \omega_2}$ (see (20) and (21)) where

$$p_1 = -R_1 X_{CP} - \frac{R_2 X_{CP}}{Q_L Q_C} - \frac{R_1 R_2}{Q_L} + R_2 X_{LS} \left(\frac{1}{Q_L^2} - 1\right) + X_{LS} X_{CP} \left(\frac{1}{Q_L} - \frac{1}{Q_C}\right) + \left(\frac{X_{LS} X_{CP}}{Q_L} + R_2 X_{CP}\right) \left(1 + \frac{1}{Q_L Q_C}\right)$$

$$q_1 = -\frac{R_1 R_2 X_{CP}}{Q_C} + R_2 X_{LS} X_{CP} \left(1 + \frac{1}{Q_L Q_C}\right)$$

$$r_1 = \left(R_2 + \frac{X_{CP}}{Q_C}\right) \left(\frac{1}{Q_L} - \frac{1}{Q_C}\right) + X_{CP} \left(1 + \frac{1}{Q_L Q_C}\right)$$

$$s_1 = \frac{2R_2 X_{CP}}{Q_C}$$

$$k_1 = -\frac{X_{CP}}{Q_C} \left(2 + \frac{1}{Q_L Q_C}\right) + \frac{X_{CP}}{Q_L} - R_2$$

$$l_1 = R_2 X_{CP} \left(1 - \frac{1}{Q_C}\right) - \frac{R_2 X_{LS}}{Q_L Q_C}$$

$$m_1 = \left(\frac{X_{LS} X_{CP}}{Q_L} + X_{CP} R_2\right) \left(\frac{1}{Q_C} - \frac{1}{Q_L}\right) - X_{CP} R_1 \left(\frac{1}{Q_C} - \frac{1}{Q_L}\right) - R_1 R_2 + \frac{2R_2 X_{LS}}{Q_L} + X_{LS} X_{CP} \left(1 + \frac{1}{Q_L Q_C}\right)$$

$$n_1 = R_2 X_{LS} X_{CP} \left(\frac{1}{Q_C} - \frac{1}{Q_L}\right) + R_1 R_2 X_{CP}$$

$$p_2 = \frac{R_2 X_{CP}}{Q_C^2} + \frac{R_2 X_{LS}}{Q_L Q_C} - X_{CP} R_2$$

$$q_2 = \frac{R_2}{Q_C} \left(-R_1 X_{CP} + \frac{X_{LS} X_{CP}}{Q_L}\right) + X_{CP} R_2 X_{LS}$$

$$r_2 = X_{CP} \left(1 - \frac{1}{Q_C^2} + \frac{2}{Q_L Q_C}\right) + R_2 \left(\frac{1}{Q_L} - \frac{1}{Q_C}\right)$$

$$s_2 = R_1 X_{CP} \left(\frac{1}{Q_C} - \frac{1}{Q_L}\right) + R_1 R_2 + \frac{X_{LS} X_{CP}}{Q_L} \left(\frac{1}{Q_L} - \frac{1}{Q_C}\right)$$

$$- \frac{2R_2 X_{LS}}{Q_L} + R_2 X_{CP} \left(\frac{1}{Q_L} - \frac{1}{Q_C}\right) - X_{LS} X_{CP} \left(1 + \frac{1}{Q_L Q_C}\right)$$

$$Z_{in} = jX_{LS} + \frac{X_{LS}}{Q_L} - jX_{CS} + \frac{X_{CS}}{Q_C} + \frac{1}{\left(\frac{1}{R_2} + \frac{1}{\left(\frac{1}{jX_{LP}} + \frac{1}{X_{LP}/Q_L}\right)} + \frac{1}{\left(-jX_{CP} + \frac{1}{X_{CP}/Q_C}\right)}\right)} \quad (19)$$

$$X_{LP}^2 (p_1 r_1 - k_1 m_1) + X_{LP} (p_1 s_1 + q_1 r_1 - k_1 n_1 - l_1 m_1) - (q_1 s_1 - l_1 n_1) = 0 \quad (20)$$

$$X_{CS}^2 (p_2 r_2 - k_2 m_2) + X_{CS} (p_2 s_2 + q_2 r_2 - k_2 n_2 - l_2 m_2) - (q_2 s_2 - l_2 n_2) = 0 \quad (21)$$

$$\begin{aligned}
k_2 &= -\frac{2R_2X_{CP}}{Q_C} \\
l_2 &= R_2X_{CP}\left(R_1 - \frac{X_{LS}}{Q_L}\right) + \frac{R_2X_{CP}X_{LS}}{Q_L} \\
m_2 &= -\frac{X_{CP}}{Q_C}\left(1 + \frac{1}{Q_LQ_C}\right) + X_{CP}\left(\frac{1}{Q_L} - \frac{1}{Q_C}\right) - R_2 \\
n_2 &= \left(R_1X_{CP} - R_2X_{CP} - \frac{X_{LS}X_{CP}}{Q_L}\right)\left(1 + \frac{1}{Q_LQ_C}\right) \\
&\quad + \frac{R_1R_2}{Q_L} + R_2X_{CP}\left(1 - \frac{1}{Q_L^2}\right) + X_{LS}X_{CP}\left(\frac{1}{Q_C} - \frac{1}{Q_L}\right)
\end{aligned}$$

Analysing the derived solution, two components (L_S and C_P) are computed assuming the network is narrow band (even though their parasitic are accounted). This may lead to performance degradation. Hence, to arrive to a more accurate solution, these two components are recalculated [(22), (23)] with respect to overall system impedance equation and utilising the above derived solution for L_P and C_S . The same procedure [used for deriving (20), (21)] is followed to derive the quadratic equations for L_S and C_P as given in (22), (23) where

$$\begin{aligned}
p_3 &= \left(-R_2 - \frac{X_{LP}}{Q_L}\right)\left(1 + \frac{1}{Q_LQ_C}\right) + X_{LP}\left(\frac{1}{Q_L} - \frac{1}{Q_C}\right) \\
q_3 &= \left(R_1X_{LP} - X_{CS}\frac{X_{LP}}{Q_C} - R_2X_{LP}\right)\left(1 + \frac{1}{Q_LQ_C}\right) \\
&\quad + \frac{R_1R_2}{Q_C} - \frac{R_1X_{CS}}{Q_C^2} + X_{CS}X_{LP}\left(\frac{1}{Q_L} - \frac{1}{Q_C}\right) + X_{CS}R_2 \\
r_3 &= R_2X_{LP}\left(\frac{1}{Q_L} - 1\right) + \frac{R_2X_{CS}}{Q_LQ_C} \\
s_3 &= R_2X_{LP}\left(X_{CS} - \frac{R_1}{Q_L}\right) \\
k_3 &= \left(R_2 + \frac{X_{LP}}{Q_L}\right)\left(\frac{1}{Q_L} - \frac{1}{Q_C}\right) - X_{LP}\left(1 + \frac{1}{Q_LQ_C}\right) \\
l_3 &= X_{LP}\left(R_1 - R_2 - \frac{X_{CS}}{Q_C}\right)\left(\frac{1}{Q_L} - \frac{1}{Q_C}\right) \\
&\quad + \frac{2R_2X_{CS}}{Q_C} + X_{CS}X_{LP}\left(1 + \frac{1}{Q_LQ_C}\right) - R_1R_2 \\
m_3 &= \frac{2X_{LP}R_2}{Q_L} \\
n_3 &= R_2X_{LP}\left(-R_1 + X_{CS}\left(\frac{1}{Q_L} - \frac{1}{Q_C}\right)\right) \\
p_4 &= \left(-R_2 - \frac{X_{LP}}{Q_L}\right)\left(1 + \frac{1}{Q_LQ_C}\right) + X_{LP}\left(\frac{1}{Q_L} - \frac{1}{Q_C}\right) \\
q_4 &= R_2X_{LP}\left(1 - \frac{1}{Q_L^2}\right) - \frac{R_2X_{CS}}{Q_LQ_C}
\end{aligned}$$

$$\begin{aligned}
r_4 &= \left(-R_1X_{LP} + X_{CS}\frac{X_{LP}}{Q_C} + R_2X_{LP}\right)\left(1 + \frac{1}{Q_LQ_C}\right) \\
&\quad - \frac{R_1R_2}{Q_C} + \frac{R_2X_{CS}}{Q_C^2} + X_{CS}X_{LP}\left(\frac{1}{Q_L} - \frac{1}{Q_C}\right) - X_{CS}R_2 \\
s_4 &= R_2X_{LP}\left(X_{CS} - \frac{R_1}{Q_L}\right) \\
k_4 &= \left(R_2 + \frac{X_{LP}}{Q_L}\right)\left(\frac{1}{Q_L} - \frac{1}{Q_C}\right) - X_{LP}\left(1 + \frac{1}{Q_LQ_C}\right) \\
l_4 &= -\frac{2X_{LP}R_2}{Q_L} \\
m_4 &= X_{LP}\left(R_2 - R_1 + \frac{X_{CS}}{Q_C}\right)\left(\frac{1}{Q_L} - \frac{1}{Q_C}\right) \\
&\quad - \frac{2R_2X_{CS}}{Q_C} - X_{CS}X_{LP}\left(1 + \frac{1}{Q_LQ_C}\right) + R_1R_2 \\
n_4 &= R_2X_{LP}\left(-R_1 + X_{CS}\left(\frac{1}{Q_L} - \frac{1}{Q_C}\right)\right)
\end{aligned}$$

A set of component values computed through the proposed method for different transformation ratios and different component quality factors are listed in Table 5. It is interesting to notice in the table that, the component values need a considerable change when their quality factor is low. More than 100% change in component values are observed for a change in component quality factor from ideal to below ten. The S_{11} plots of the networks using these components are shown in Fig. 10 for high to low and low to high matching networks. The result shows that the proposed design method enhances the matching performance substantially.

The solution for dual-band network designed and validated here is assuming the load impedance to be equal at both the frequencies. However, this method can be applied for networks having unequal load impedances at two frequencies. In order to obtain favourable solution on this scenario, a common impedance value has to be identified by relating the two load impedance values with appropriate relationship factor. Also, the difference between the two frequencies is to be taken care. This procedure is tested in the proposed method. However, to derive a generic solution in this scenario is another research problem.

7 Measurements and result validation

7.1 Measurement results

The proposed design technique is validated through simulations and measurements using UMC180 nm RFCMOS process libraries. Simulations are done using Cadence SpectreRF tools. On-chip spiral inductors and metal-insulator-metal capacitors are used for validation. The available range of on-chip inductor for this technology (UMC0.18 μm) ranges from 0.6 to 14 nH and quality factor in the range of 5–10. Accounting for the Q -values of passives components from PDK documents, the derived inductor and capacitor values for different matching networks to match from 20 to 50 Ω at 1.8 GHz are given in Table 6. Among the L, Pi, and T networks, the Pi network is fabricated and tested as a case study. A network to transform 5–50 Ω at 0.9 and 1.8 GHz (given in Table 6) is considered for dual-band implementation.

The fabricated die photograph of Pi and dual-band L-networks are shown in Figs. 11a and c, respectively. Die characterisation is performed using Cascade Microtech vacuum probe station, PLV50 and Agilent VNA, PNA-X N5244A. The measured S_{11} and S_{21}

$$X_{LS}^2(p_3r_3 - k_3m_3) + X_{LS}(p_3s_3 + q_3r_3 - k_3n_3 - l_3m_3) - (q_3s_3 - l_3n_3) = 0 \quad (22)$$

$$X_{CP}^2(p_4r_4 - k_4m_4) + X_{CP}(p_4s_4 + q_4r_4 - k_4n_4 - l_4m_4) - (q_4s_4 - l_4n_4) = 0 \quad (23)$$

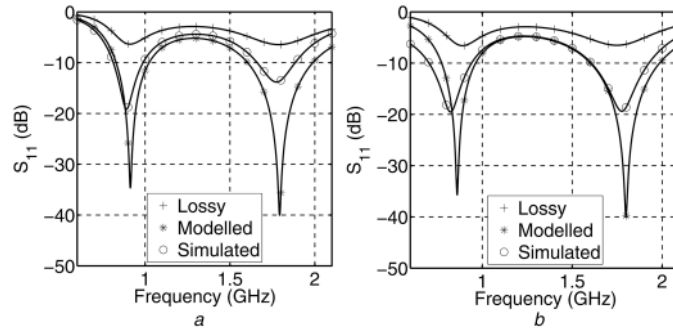


Fig. 10 Modelled and simulated S_{11} response using the proposed method
(a) High to low (500–50 Ω), (b) Low to high (50–50 Ω)

Table 5 Components using the proposed method at 0.9 and 1.8 GHz

Q_L, Q_C	High to low				Low to high			
	L_S , nH	C_S , pF	L_P , nH	C_P , pF	L_S , nH	C_S , pF	L_P , nH	C_P , pF
∞, ∞	26.5	0.59	14.8	1.06	2.65	5.89	1.47	10.6
5, 30	10.6	1.47	6.17	2.53	5.51	2.83	3.86	4.04

Table 6 Derived component values for UMC 0.18 μm technology for 1.8 GHz (0.9 and 1.8 GHz for dual band)

CKT	Q_L	L_L , nH	L_R , nH	C_L , pF	C_R , pF
L-match	3.6	2.226	—	1.634	—
Pi-match	3.6	1.45	0.303	4.728	24.98
T-match	3.6	9.58	18.82	0.792	0.363
dual band	3.6	5.51	2.83	3.86	4.04

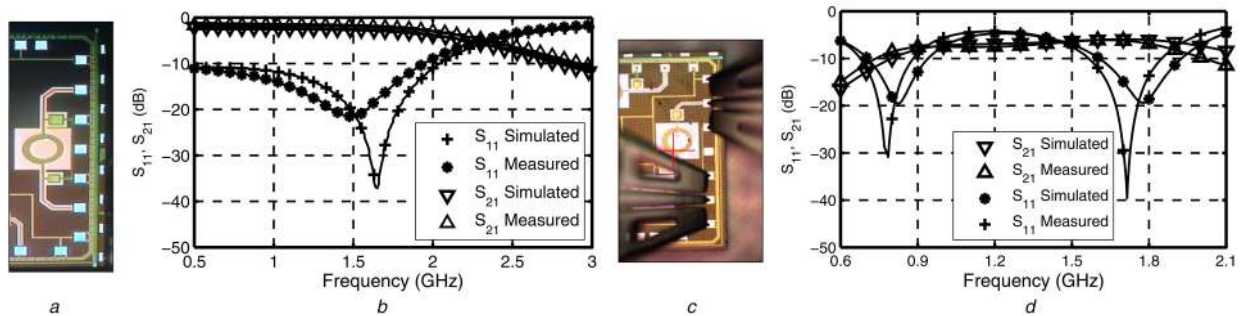


Fig. 11 Die photograph and measured S -parameters results

(a) Die photograph of Pi network, (b) S -parameters of Pi network, (c) Die photograph of dual-band L-network, (d) S -parameters of dual-band L-network

results for Pi and dual-band L-networks are shown in Figs. 11b and d, respectively. The measured results are closer to the results achieved from max–max (inductor–capacitor) corner simulation. The difference between measured and simulated results (<5%) is due to the effect of connecting traces from the circuit to the pad. In real on-chip application circuits, the matching network becomes integral part of the load. Considering the geometry of on-chip interconnects, load side reflection is least critical. Therefore, the proposed Q -factor aware analytical design technique has been proven and will be useful for low power RF circuit design.

7.2 Discussion

The measured S_{11} and S_{21} performances of the proposed matching networks are close to simulated results. The S_{11} is much enhanced and almost closer to ideal component performance. However, due to losses in the low- Q components, the insertion loss exist in the network and hence, the S_{21} is little degraded [18]. Insertion loss in dual-band network is comparatively higher than single-frequency network because the former uses two low Q inductors (net loss is more) compared with only one in the later. The insertion loss can be minimised through improving the component Q -factor. The stop-band attenuation in the presence of lossy components may be increased by adding a notch circuit [1] at appropriate frequency in the successive blocks (mostly needed in dual-band network).

Table 7 shows a consolidated list of different impedance matching techniques proposed in literatures. Complexity level given in Table 7 is considered in terms of hardware requirement. The proposed design method has no additional hardware requirement and has less computational complexity.

The proposed method can be used for designing matching networks even if the source or load impedance is complex (having reactance). To do this, the type of matching network should be chosen in such a way that the reactive part of load (or source) can be absorbed into the network as a component (or part of). This method is feasible only if the reactance of load (or source) at the matching frequency is lesser than or equal to that of the sharing (or replacing) component in the network.

8 Conclusion

A parasitic aware analytical design method for on-chip single and dual-frequency matching networks incorporating the component non-idealities is proposed. This method gives very accurate matching performance even with low Q -factor components and eliminates the need of component tuning. The method is validated for different frequencies through simulations and die measurements.

Table 7 Consolidation of impedance matching techniques

Year, ref.	Network	F_{\max}	Implementation	Technique	Complexity
2006 [4]	L	100 MHz ^a	PCB	analytical	low
2011 [10]	distributed	660 MHz	—	hardware reconfigurable	high
2010 [11]	L	—	—	hardware reconfigurable	high
2010 [12]	L, transformer	3.85 GHz ^a	on-chip	analytical	high
2011 [13]	Pi	403 MHz ^a	on-chip	hardware reconfigurable	high
this work	L, Pi, T, dual	1.8 GHz ^a	on-chip	analytical	low

^aMeasured frequency.

9 References

- [1] Bowick, C.: 'RF circuit design' (Howard W. Sams, London, UK, 1985)
- [2] Dutta Roy, S.C.: 'Characteristics of single- and multiple-frequency impedance matching networks', *IEEE Trans. Circuits Syst. II: Express Briefs*, 2015, **62**, (3), pp. 222–225
- [3] Asgaran, S., Jamal Deen, M., Chen, C.-H.: 'Design of the input matching network of RF CMOS LNAs for low-power operation', *IEEE Trans. Circuit Syst. I: Regul. Pap.*, 2007, **54**, (3), pp. 544–554
- [4] Han, Y., Perreault, D.J.: 'Analysis and design of high efficiency matching networks', *IEEE Trans. Power Electron.*, 2006, **21**, (5), pp. 1484–1491
- [5] Chung, B.K.: 'Q-based design method for T network impedance matching', *Microelectron. J.*, 2006, **37**, (9), pp. 1007–1011
- [6] Becciolini, B.: 'Motorola application note: impedance matching networks applied to RF power transistors'. Available at http://www.rfwireless.rell.com/pdfs/AN_721_D.pdf, 1993
- [7] Lee, T.H.: 'Design of CMOS radio-frequency integrated circuits' (Cambridge University Press, UK, 2004, 2nd edn.)
- [8] Thompson, M., Fidler, J.K.: 'Determination of impedance matching domain of impedance matching networks', *IEEE Trans. Circuits Syst. I, Regul. Pap.*, 2004, **51**, (10), pp. 2098–2106
- [9] Serban, A., Karlsson, M., Gong, S., *et al.*: 'Component tolerance effect on ultra wideband low noise amplifier performance', *IEEE Trans. Adv. Packag.*, 2010, **33**, (3), pp. 660–668
- [10] Sanchez-Perez, C., de Mingo, J., Garcia-Ducar, P., *et al.*: 'Dynamic load modulation with a reconfigurable matching network for efficiency improvement under antenna mismatch', *IEEE Trans. Circuits Syst. II, Express Briefs*, 2011, **58**, (12), pp. 892–896
- [11] Bezooijen A, Van, de Jongh, M.A., van Straten, F., *et al.*: 'Adaptive impedance-matching techniques for controlling L networks', *IEEE Trans. Circuits Syst.*, 2010, **57**, (2), pp. 495–505
- [12] Soltani, N., Yuan, F.: 'A high-gain power-matching technique for efficient radio-frequency power harvest of passive wireless microsystems', *IEEE Trans. Circuits Syst. I, Regul. Pap.*, 2010, **57**, (10), pp. 2685–2695
- [13] Po, F.C.W., de Foucauld, E., Morche, D., *et al.*: 'A novel method for synthesizing an automatic matching network and its control unit', *IEEE Trans. Circuit Syst.: Regul. Pap.*, 2011, **58**, (9), pp. 2225–2236
- [14] Lizhong Zhu, C.S., Boxiu, W.: 'Lumped lossy circuit synthesis and its application in broad-band FET amplifier design in MMICs', *IEEE Trans. Microw. Theory Tech.*, 1989, **37**, (9), pp. 1488–1491
- [15] Liu, L., Ku, W.: 'Computer-aided synthesis of lumped lossy matching networks for monolithic microwave integrated circuits (MMICs)', *IEEE Trans. Microw. Theory Tech.*, 1984, **32**, (3), pp. 282–289
- [16] Dasgupta, K., Dutta, A., Bhattacharya, T.K.: 'Parasitic aware impedance matching technique for RF amplifiers', *Analog Integr. Circuit Signal Process.*, 2012, **70**, pp. 91–102
- [17] Nallam, N., Chatterjee, S.: 'Multi-band frequency transformations, matching networks and amplifiers', *IEEE Trans. Circuits Syst. I, Regul. Pap.*, 2013, **60**, (6), pp. 1635–1647
- [18] Niknejad, A.M.: 'Electromagnetics for high-speed analog and digital communication circuits' (Cambridge University Press, UK, 2007)